TOXICOLOGICAL SCIENCES **125(2)**, 496–508 (2012)
doi:10.1093/toxsci/kfr313
Advance Access publication November 17, 2011

Subchronic Polychlorinated Biphenyl (Aroclor 1254) Exposure Produces Oxidative Damage and Neuronal Death of Ventral Midbrain Dopaminergic Systems

Donna W. Lee,* Sarah A. Notter,* Mona Thiruchelvam,† Daniel P. Dever,* Richard Fitzpatrick,‡ Paul J. Kostyniak,‡ Deborah A. Cory-Slechta,* and Lisa A. Opanashuk*,[1]

*Department of Environmental Medicine, School of Medicine and Dentistry, University of Rochester, Rochester, New York 14642; †Environmental and Occupational Health Science Institute, University of Medicine and Dentistry of New Jersey, Piscataway, New Jersey 08854; and ‡Department of Pharmacology and Toxicology, School of Medicine and Biomedical Sciences, State University of New York at Buffalo, Buffalo, New York 14214

[1]To whom correspondence should be addressed at Department of Environmental Medicine, School of Medicine and Dentistry, University of Rochester, Box EHSC Rochester, NY 14642. Fax: (585) 256-2591. E-mail: lisa_opanashuk@urmc.rochester.edu.

Received September 2, 2011; accepted November 11, 2011

Recent epidemiologic studies have demonstrated a link between organochlorine and pesticide exposure to an enhanced risk for neurodegenerative disorders such as Parkinson's disease (PD). A common biological phenomenon underlying cell injury associated with both polychlorinated biphenyl (PCB) exposure and dopaminergic neurodegeneration during aging is oxidative stress (OS). In this study, we tested the hypothesis that oral PCB exposure, via food ingestion, impairs dopamine systems in the adult murine brain. We determined whether PCB exposure was associated with OS in dopaminergic neurons, a population of cells that selectively degenerate in PD. After 4 weeks of oral exposure to the PCB mixture Aroclor 1254, several congeners, mostly *ortho* substituted, accumulated throughout the brain. Significant increases in locomotor activity were observed within 2 weeks, which persisted after cessation of PCB exposure. Stereologic analyses revealed a significant loss of dopaminergic neurons within the substantia nigra and ventral tegmental area. However, striatal dopamine levels were elevated, suggesting that compensatory mechanisms exist to maintain dopamine homeostasis, which could contribute to the observed increases in locomotor activity following PCB exposure. Biochemical experiments revealed alterations in OS markers, including increases in SOD and HO-1 levels and the presence of oxidatively modified lipids and proteins. These findings were accompanied by elevated iron levels within the striatal and midbrain regions, perhaps due to the observed dysregulation of transferrin receptors and ferritin levels following PCB exposure. In this study, we suggest that both OS and the uncoupling of iron regulation contribute to dopamine neuron degeneration and hyperactivity following PCB exposure.

Key Words: **organochlorines; oxidative stress; Parkinson's disease; neurodegeneration; iron; environment.**

Polychlorinated biphenyls (PCBs), synthetic members of the halogenated aromatic hydrocarbon family, are ubiquitous in the environment due to their improper disposal and resistance to degradation (Tilson and Kodavanti, 1997). Chronic PCB exposure during adulthood can lead to a variety of human health problems, including liver damage, dermal lesions, immunodeficiency, and endocrine damage (Hsu *et al.*, 1985). Moreover, delays in psychomotor development and lowered test scores on IQ and behavioral assessments have been observed in children perinatally exposed to PCBs (Hsu *et al.*, 1985; Kashimoto *et al.*, 1981). Although the precise neurological consequences in adult humans have not been completely defined, increasing evidence suggests that PCB exposure is associated with enhanced risk for impaired brain function.

Support for a relationship between organochlorine exposure and neurodegeneration was provided by a study that reported elevated levels of several PCB congeners in postmortem brain tissue from patients with Parkinson's disease (PD) (Corrigan *et al.*, 1998). A more recent study demonstrated a positive correlation between consumption of PCB-loaded whale meat and blubber during adult life and PD (Petersen *et al.*, 2008). Additionally, a retrospective mortality study based on PCB-exposed workers revealed a significant incidence of PD and dementia in women exposed to high levels of the toxicant (Steenland *et al.*, 2006). Together, these findings provide further rationale for precisely defining the adverse neurological consequences of PCB exposure during adulthood.

Although the specific mechanisms of PCB neurotoxicity have not been precisely defined, dopaminergic (DAergic) pathways, known to play important roles in motor function (Rousselet *et al.*, 2003), have been identified as targets of PCB-mediated damage. PCBs have been shown to disrupt dopamine (DA) homeostasis both *in vivo* (Seegal *et al.*, 2002) and *in vitro* (Lee and Opanashuk, 2004), but the mechanisms by which neurons are injured remain undefined. Depending upon the exposure conditions, PCBs have been shown to produce either

increases in extracellular DA (Bemis and Seegal, 2004; Seegal *et al*., 2002) or decreases in tissue DA (Seegal, 1994). Our previous work revealed that exposure to Aroclor 1254 (A1254), a PCB mixture, led to decreased intracellular DA and increased turnover in dopaminergic (DAergic) cells *in vitro* (Lee and Opanashuk, 2004). Because DA is capable of undergoing autoxidation, which leads to the generation of reactive oxygen species (ROS), there is an increased risk for cellular damage if its levels are not properly managed (Berman and Hastings, 1999). Moreover, ROS are produced during DA synthesis and metabolism (Graham, 1978; Tse *et al*., 1976). If not buffered by cellular antioxidant defense systems, enhanced ROS levels derived from DA metabolism or alternative cellular sources could produce macromolecular injury in sensitive neuronal populations following PCB exposure.

The connection between an oxidative stress (OS) response and nervous system damage following PCB exposure during adulthood has received very little attention. Because free radical generation increases during the normal aging process and ROS are thought to be involved in the pathogenesis of several neurological disorders (Jenner, 1996), exposure to prooxidant environmental chemicals could accelerate the onset or progression of neurodegenerative diseases. Iron is essential for maintaining numerous cellular functions, but its highly reactive nature stimulates hydroxyl radical production via the Fenton/Haber-Weiss reactions (Halliwell, 1992) that could be detrimental to neurons and other cells in the central nervous system (CNS). Disrupted iron homeostasis has been demonstrated in neurodegeneration (Smith *et al*., 2004) and hypoxic-ischemic models (Palmer *et al*., 1999). In rodents, PCB exposure resulted in enhanced hepatic porphyria in iron-loaded mice (Madra *et al*., 1996) and elevated iron levels in rat hepatocytes (Whysner and Wang, 2001). Additionally, we determined that iron chelation and inhibition of HO-1 by tin protoporphyrins were sufficient to prevent the PCB-induced accumulation of iron in a DAergic cell culture model (Lee *et al*., 2006), suggesting that disrupted iron homeostasis may contribute to ROS production and neurotoxicity.

Although the sources of ROS in response to PCB exposure remain unknown, OS could be a primary mediator of neuronal injury or death following PCB exposure. As suggested above, exposure to PCBs and other prooxidant agents during adulthood could accelerate or exacerbate neurodegenerative events. Therefore, the central aim of this study was to test the hypothesis that PCB accumulation in the brain leads to OS, which mediates DAergic neuronal injury and abnormal motor function following subchronic PCB exposure. A corollary to this hypothesis is that the increased iron levels following PCB exposure contributes to neurotoxicity *in vivo*. This study demonstrates that adult mice exposed to PCBs exhibit hyperactivity, abnormal DA homeostasis, and a widespread OS response in the brain. Furthermore, increased iron deposition was observed in the nigrostriatal DA region of PCB-exposed mice. Notably, these effects were accompanied by neuronal loss in the ventral midbrain (VMB). Therefore, PCB exposure during adulthood should be considered as an environmental risk factor that might predispose neurons to further oxidative damage during normal aging and neurodegenerative processes such as PD.

MATERIALS AND METHODS

Reagents. All chemicals were purchased from Sigma (St Louis, MO), unless otherwise stated. Aroclor 1254 (Lot 124–191; 99% purity) was purchased from AccuStandard Inc. (New Haven, CT).

Animals. Male C57BL/6 mice (8 weeks old) were purchased from Taconic Farms (NY) and individually housed with food and water available *ad libitum* in a room maintained under constant temperature and humidity with a 12:12 light-dark cycle. Singly caged mice were habituated to the *vivarium* for 1 week prior to commencement of experiments and were weighed at the end of week 2 and 4 of treatment and again 2 weeks postexposure. All animals were cared for and treated in accordance with the National Institutes of Health and University of Rochester Animal Care and Use Committee guidelines.

PCB exposure. Because PCBs were commercially manufactured as Aroclor chemical mixtures in the United States, humans are more likely to have been exposed to multiple rather than individual PCB congeners. Therefore, mice were exposed to an Aroclor mixture of PCBs. Four groups of C57BL/6 mice ($n = 20$ per group) were fed daily one-fourth of a vanilla wafer cookie (Nabisco) containing either 200 µl of vehicle (soybean oil), 6, 12, or 25 mg/kg Aroclor 1254 for 4 weeks. The mice were then allowed to recover for 2 weeks before sacrifice. Although it is difficult to extrapolate the relevance of animal dosing to human body burden, these doses were chosen based on previous studies showing accumulation of PCBs within the brain in the low micromolar concentration range following a 30 mg/kg/day exposure regimen for 30 days (Kodavanti *et al*., 1998). Additionally, in our previous *in vitro* studies, the effects of PCBs on DAergic systems occurred within the micromolar range, supporting the utilization this dose range for this study (Lee and Opanashuk, 2004). There was no significant impact on body weights between the different PCB exposure groups throughout the course of the study.

Determination of PCB congener profiles in the rat brain tissues. Congener-specific analysis of rat brain tissues was performed at the Toxicology Research Center, State University of New York at Buffalo based upon the methods described by Greizerstein *et al*. (1997). Briefly, rat brain tissues were weighed and transferred to a glass vial containing 2 ml hexane (gas chromatography [GC]-mass spectrometry grade; Burdick & Jackson, Morristown, NJ). Congeners 46 and 142 were added as surrogate standards to each tissue samples. Each sample vial was vortexed for 5 min, followed by 2 × 15 min sonication (Branson Model 3510; Danbury, CT) at room temperature. The 2 ml hexane extract was loaded to preconditioned Florisil Sep-Pak cartridge (500 mg; Waters, Milford, MA) and eluted with 10 ml hexane. The eluent was collected in a TurboVap tube and concentrated to 0.2 ml by TurboVap II evaporator (Zymark, Hopkinton, MA). Congeners 30 and 204 were added as internal standards prior to gas chromatographic analysis. The Agilent 6890 Gas Chromatograph (Palo Alto, CA) was equipped with electron capture detection (ECD), temperature and electronic pressure programming capabilities, and a splitless injector. Separation of individual PCB congeners was performed using a 60 m SPB-5 fused silica capillary column (0.25 mm inner diameter, 0.25-µm film thickness) from Supelco (Bellefonte, PA). The GC data were acquired and quantified using Agilent ChemStation software. Identification and quantification of the individual congeners were performed by comparison with reference standards. The analytes were identified by their retention times relative to the respective internal standards (congener 30 for peaks eluting before congener 101 and congener 204 for congener 101 and those eluting thereafter). Calibration curves (second order polynomial) were generated based upon dilutions of an Environmental Protection Administration (EPA) PCB Congener Calibration Check solution (Ultra Scientific No. RPC-EPA) for quantification of congeners 8, 18, 28, 44, 52, 66, 77, 101, 105, 118, 126,

128, 138, 153, 170, 180, 187, 195, and 206. The concentrations of congeners not present in the EPA calibration standard were calculated using average response factors generated in the TRC laboratory, determined from individual congener reference standards. The results from the GC analysis were exported to an Excel spreadsheet, where they were corrected (blank subtracted) for the mean concentration of each congener determined in the control tissue samples. Results were also adjusted for the recovery of surrogates (46, 142) added to each sample.

Locomotor activity. Automated locomotor activity chambers (Opto-Varimex Minor; Columbus Instruments, Columbus, OH) were used to quantify locomotor activity. The activity chambers were equipped with one set each of the infrared photo beams (3 mm in diameter) on the horizontal and vertical planes. Beam breaks were recorded each minute for 45 min for horizontal (breaking of sequential horizontal photobeams), vertical (breaking of vertical plane photobeams), and ambulatory (breaking of any, including repeated, horizontal photobeam) movements. Mice were initially habituated to three 1 h sessions during the acclimation period prior to feeding with experimental cookies. Motor activity was assessed at the start of the experiment as well as at the end of weeks 2, 4, and 2 weeks postexposure.

Dopamine and metabolite analyses by high-performance liquid chromatography. Neurotransmitter concentrations were measured in striatal lysates by high-performance liquid chromatography (HPLC). Striatal sections were dissected and placed in harvesting buffer containing 500mM sodium acetate, 400mM sodium perchlorate, 2mM EDTA, and 0.01% (vol/vol) glacial acetic acid before processing and neurochemical analyses (Gwiazda *et al*., 2002; Lee and Opanashuk, 2004). Eluted peaks from samples were analyzed for peak area, and concentrations of each compound were extrapolated from a standard curve. DA turnover was determined by dividing (dihydroxyphenylacetic acid [DOPAC]) + (homovanillic acid [HVA]) by [DA].

Immunohistochemistry for tyrosine hydroxylase, dopamine transporter, and stereology. At least seven animals per exposure group were perfused with heparinized saline and 4% paraformaldehyde (PFA) before brain removal and postfixation in 4% PFA for 7 days before transfer into graded sucrose solutions (10–30%). The PFA-fixed brains were then coronally cut into 30-μm sections on a freezing sliding microtome and collected in cryoprotectant and stored at −20°C until ready for immunostaining. Sections containing the striatal and substantia nigra regions were rinsed in PBS containing 0.3% Triton and blocked with 10% normal goat serum (in PB-Triton) prior to incubation with a rabbit polyclonal anti-tyrosine hydroxylase (TH) primary antibody (ST and SN, 1:4000; Chemicon, Temecula, CA) and counterstained with cresyl violet following TH staining or with a mouse monoclonal anti-dopamine transporter (DAT) primary antibody (ST, 1:1000; Chemicon). Striatal sections stained with TH or DAT primary antibodies were subject to densitometric analysis using Scion Image. Additionally, the total number of TH-positive and TH-negative (Nissl positive but TH-negative) neurons in the substantia nigra pars compacta (SNpc) and the ventral tegmental area (VTA) were stereologically counted in 7–8 mice pergroup using the optical fractionator method (Thiruchelvam *et al*., 2003).

Lipid peroxidation assay. Peroxidation of polyunsaturated fatty acids and esters of cellular membranes can lead to the production of aldehydes, such as malondialdehyde (MDA) and 4-hydroxy-nonenal (4-HNE), which can alter membrane function and integrity. Therefore, to determine lipid peroxide by-products, this study utilized a chromogenic reagent that reacts and condenses with MDA and 4-HNE at 45°C to form a stable chromophore with maximal absorbance at 586 nm (Calbiochem, La Jolla, CA).

Protein oxidation assay. Although different protein modifications result in a variety of functional consequences, the accumulation of protein carbonyl is mainly associated with dysfunction of cellular protein function. This assay takes advantage of these carbonyl groups for the detection of oxidatively modified proteins (OxyBlot; Chemicon). Cellular extracts (~5 μg) were diluted 1:1 with 12% SDS before the derivatization of carbonyl groups on the protein side chains by 2,4-dinitrophenylhydrazine (DNPH) at room temperature for 15 min. The protein samples were then separated on 10% SDS-polyacrylamide gel electrophoresis (PAGE) gels and transferred onto polyvinylidene difluoride (PVDF) membranes, which were probed with primary antibodies specific to the DNP moiety of the proteins (1:300). Protein bands were detected by chemiluminescence substrate for horseradish peroxidase–conjugated secondary antibodies (LumiGlo; KPL, Gaithersburg, MD). Subsequently, densitometric readings of each lane were quantified using Quantity One analysis software (The Discovery Series; Bio-Rad, Hercules, CA).

Two-dimensional isoelectric focusing/SDS-PAGE analysis. Striatal and cerebellar sections were dissected out and homogenized in the following buffer (50 mg/ml): 30mM Tris-HCl, 7M urea, 0.4% [(3-cholamidopropyl)-dimethyl-ammonio]1-propanesulfonate (CHAPS), 2mM PMSF, and antiprotease cocktail (100mM AEBSF, 0.08mM aprotinin, 2mM leupeptin, 1.5mM pepstatin A, 4mM bestatin, and 1.4mM E-64; Sigma). Total protein was quantified with the MicroBCA protein assay (Pierce, Rockford, IL). Equal amounts (100 μg) of protein were subject to acetone precipitation prior to resuspension with the isoelectric focusing (IEF) sample loading buffer (200 μl final volume) that consisted of the following: 7M urea, 2M thiourea, 50mM dithiothreitol (DTT), 4% CHAPS, 0.2% carrier ampholytes, and 0.002% (wt/vol) bromophenol blue. Tissue samples were then loaded onto pH 3–10 immobilized pH gradient (IPG) strips (11 cm) and allowed to passively rehydrate at room temperature for 3 h prior to active rehydration at 50 V for 20 h using the PROTEAN IEF cell (Bio-Rad). Following IPG strip rehydration, IEF was performed under a slow ramping mode to achieve 80,000 V h (fixed current limit at 50 μA per strip). Prior to the two dimension (2D) of SDS-PAGE, focused IPG strips were allowed to equilibrate in base buffer containing DTT (2%) followed by base buffer containing iodoacetamide (2.5%). The equilibration base buffer consisted of 6M urea, 2% SDS, 0.05M Tris-HCl, and 20% glycerol. Twelve 2D gels were run simultaneously on Bio-Rad's DODECA cells using Tris-HCl precast gels (10% resolving and 4% stacking), followed by transfer of proteins onto PVDF membranes or direct silver staining of gels (Silver Stain Plus; Bio-Rad). The PVDF membranes were then blocked with 0.3% PBS-Tween solution containing 5% nonfat milk before incubation with the following antibodies: HO-1 (1:2000; StressGen), MnSOD (1:7500; BD Transduction Labs), CuZnSOD (1:5000; Santa Cruz Biotech), and actin (1:6000; Sigma). Protein spots were detected by chemiluminescence substrate for horseradish peroxidase–conjugated secondary antibodies and subsequently quantified using Quantity One analysis software (The Discovery Series; Bio-Rad).

Atomic absorption spectroscopy. To determine total Fe levels, cellular extracts (1 mg of protein) were digested in concentrated nitric acid (HNO_3) at 90°C in ultraclean Teflon vials before resuspension and dilution to a final concentration of 2% HNO_3 for AA analysis. Samples were analyzed on a Perkin-Elmer AA600 Graphite Furnace atomic absorption spectrometer with a Zeeman background correction. Samples were measured using a single element (Fe) lamp after a pyrolysis (1300°C) and atomization (2150°C) step. A matrix modifier solution of $Mg(NO_3)_2$ was used before readings were taken at a wavelength of 248.3 nm. The estimated limit of detection was 1.542 ng/ml.

Histochemical detection of iron. Free-floating sections (30 μm) from PFA-fixed brains were stained by a modified Perl's reaction that included an intensification step with 3,3′-diaminobenzidine (DAB), as previously reported (Palmer *et al*., 1999). The sections were first rinsed with PBS before incubation with 7% potassium ferrocyanide/3% hydrochloric acid for 1 h at room temperature and were subsequently incubated with 0.75 mg/ml DAB and 0.015% H_2O_2 until brown reaction products were observed. The sections were then rinsed in PBS prior to dehydration and cover slipped with Cytoseal.

Immunoblot analysis. Striatal tissues were homogenized in PBS containing 0.1% Triton X-100 and antiprotease cocktail (Sigma). Protein concentrations were determined by the MicroBCA assay (Pierce). Proteins (20 μg) were separated on 10% acrylamide gels and transferred to Immuno-Blot PVDF membranes (Bio-Rad). Membranes were blocked with 5% powdered milk containing 0.03% Tween-20 and probed with antibodies specific for ferritin H (1:500; Ramco Laboratories, Stafford, TX) or transferrin receptor (1:5000; Zymed Laboratories, San Francisco, CA) overnight at 4°C. Membranes were then probed with the appropriate horseradish peroxidase–conjugated secondary antibodies (1:2500; KPL) for 45 min at room temperature. Proteins were

TABLE 1
PCB (Aroclor 1254) Congener Distribution in Brain

PCB congener (LD ng/mg tissue)	STR	FCTX	CBL	VMB
2,2′,4,4′,5 (99) (0.0088)	0.0497 ± 0.0200	0.0402 ± 0.0088	0.0363 ± 0.0073	0.0626 ± 0.0145
2,3,3′,4,4′ (105) (0.0003)	0.0970 ± 0.0256	0.0779 ± 0.0081	0.0689 ± 0.0157	0.1226 ± 0.0174
2,3,4,4′,5 (114) (0.0060)	0.0088 ± 0.0006	0.0091 ± 0.0002	0.0066 ± 0.0008	0.0103 ± 0.0023
3,3′,4,4′,5 (126) (0.0059)	0.0064 ± 0.0002	0.0086 ± 0.0013	0.0066 ± 0.0004	0.0098 ± 0.0018
2,2′,3,3′,4,4′ (128) (0.0002)	0.0284 ± 0.0101	0.0227 ± 0.0058	0.0194 ± 0.0037	0.0360 ± 0.0084
2,2′,4,4′,5,5′ (153) + 2,2′,3,3′,4,6′ (132) (0.0093)	0.2834 ± 0.0256	0.2353 ± 0.0593	0.2163 ± 0.1008	0.3771 ± 0.0584
2,2′,3,3′,4,4′,6 (171) + 2,3,3′,4,4′,5 (156) (0.0000)	0.0054 ± 0.0011	0.0185 ± 0.0272	0.0032 ± 0.0010	0.0308 ± 0.0340
2,2′3,3′,4,5,6,6′ (200) + 2,3,3′,4,4′,5′ (157) (0.0128)	0.0139 ± 0.0000	0.0179 ± 0.0046	< LOD ± 0.0000	0.0225 ± 0.0107
2,3′,4,4′,5,5′ (167) (0.0005)	0.0167 ± 0.0008	0.0128 ± 0.0032	0.012 ± 9 0.0036	0.0226 ± 0.0042
2,2′,3,3′,4,5,5′ (172) (0.0007)	0.0118 ± 0.0037	0.0086 ± 0.0081	0.0070 ± 0.0025	0.0168 ± 0.0015
2,2′,3,4,4′,5,5′ (180) (0.0259)	0.064 ± 10.0069	0.0486 ± 0.0202	0.0414 ± 0.0143	0.0748 ± 0.0222
2,2′,3,4,4′,5′,6 (183) (0.0018)	0.0099 ± 0.0009	0.0079 ± 0.0020	0.0072 ± 0.0018	0.0128 ± 0.0034
2,2′,3,4′,5,6,6′ (188) (0.0002)	0.0676 ± 0.0310	0.0535 ± 0.0211	0.0226 ± 0.0005	0.1724 ± 0.0817
2,3,3′,4,4′,5,5′ (189) (0.0064)	0.0152 ± 0.0005	< LD	< LD	0.0329 ± 0.0013
2,2′,3,3′,4,4′,5,6 (195) (0.0066)	< LD	< LD	< LD	0.0260 ± 0.0003
2,3′,4,4′,5 (118) (0.0016)	0.2564 ± 0.0574	0.2073 ± 0.0244	0.2029 ± 0.0528	0.3396 ± 0.0452
2,2′,3,4,4′,5′ (138) + 2,3,3′,4′,5,6 (163) (0.0071)	0.3966 ± 0.0416	0.3275 ± 0.0792	0.2093 ± 0.0000	0.5134 ± 0.0721

Notes. CBL, cerebellum; FCTX, frontal cortex; STR, striatum; LD, limit of detection. Brain tissue samples from vehicle and 25 mg/kg A1254-exposed mice ($n = 3$) were analyzed for congener distribution. All tissue samples were corrected for background levels of PCBs, and data are mean ± SEM. Tabulated values are the detectable accumulation of PCB congeners after normalization from vehicle-treated samples, whereby the mean concentration of each congener determined in the control tissue samples was subtracted from PCB-exposed samples. Data are expressed as (nanogram PCB)/(milligram tissue). LD values (nanogram per milligram tissue) are noted next to or below each PCB congener.

visualized using a chemiluminescent substrate (KPL). All immunoblots were reprobed with β-actin (1:1000; Sigma) to confirm equal protein loading. Bands were quantified using Image J software.

Statistical analysis. For biochemical outcomes, statistical differences were analyzed by ANOVAs with treatment as a between groups factor, whereas analyses of locomotor activity data were analyzed using repeated measures ANOVAs (RMANOVAs) with treatment as a between groups factor and time as the within group factor using StatView version 5.0 (SAS Institute, Cary, NC). In the event of significant main effects or of interactions (RMANOVA), subsequent *post hoc* comparisons of mean values were by Fisher's protected least significant difference as appropriate, and statistical differences were considered significant with a p value of < 0.05.

RESULTS

PCB Congener Analysis and Accumulation

Although congener composition of A1254 (Lot 124–191) has been previously analyzed (Kodavanti *et al*., 2001), the extent of PCB accumulation and congener distribution following subchronic exposure ($\leq$ 25 mg/kg A1254) has not been studied in mice. Therefore, four separate brain regions (striatum, frontal cortex, cerebellum, and midbrain) from mice exposed to 0 or 25 mg/kg A1254 were analyzed for PCB congener analysis using GC/ECD. The highly chlorinated *ortho*-substituted congeners (PCB 118, 138 + 163, 153 + 132, 163, 180, and 188) were predominantly distributed in all brain regions (Table 1). PCB accumulation was evident throughout all of the brain regions analyzed (Fig. 1; VMB 1.895, STR 1.3682, FCTX 1.1083, CBL 0.6719 ng total PCBs/mg tissue).

PCB Exposure Increases Locomotor Activity

In the present investigation, mice exposed to 12 and 25 mg/kg A1254 exhibited significant increases in vertical activity counts at the end of 2 weeks that were further elevated by the end of 4 weeks of exposure. After cessation of PCB exposure, higher vertical activity counts persisted with the 12 and 25 mg/kg dose groups and were observed in the lowest 6 mg/kg dose group (Fig. 2A; main effect of exposure $F_{3,99} = 17.976$, $p < 0.0001$ and interaction effect of time and exposure $F_{3,99} = 5.799$, $p < 0.0001$).

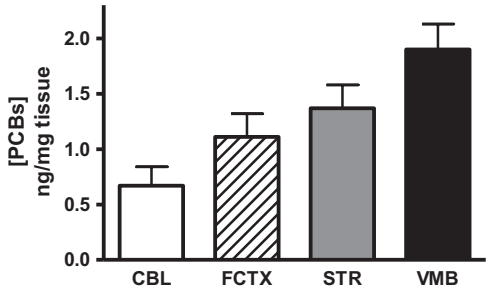

FIG. 1. Regional accumulation of PCBs within the brain. Brain tissue samples (CBL: cerebellum; FCTX: frontal cortex; VMB; and STR: striatum) from A1254-exposed mice ($n = 3$) were handled and processed exactly as described in Table 1.

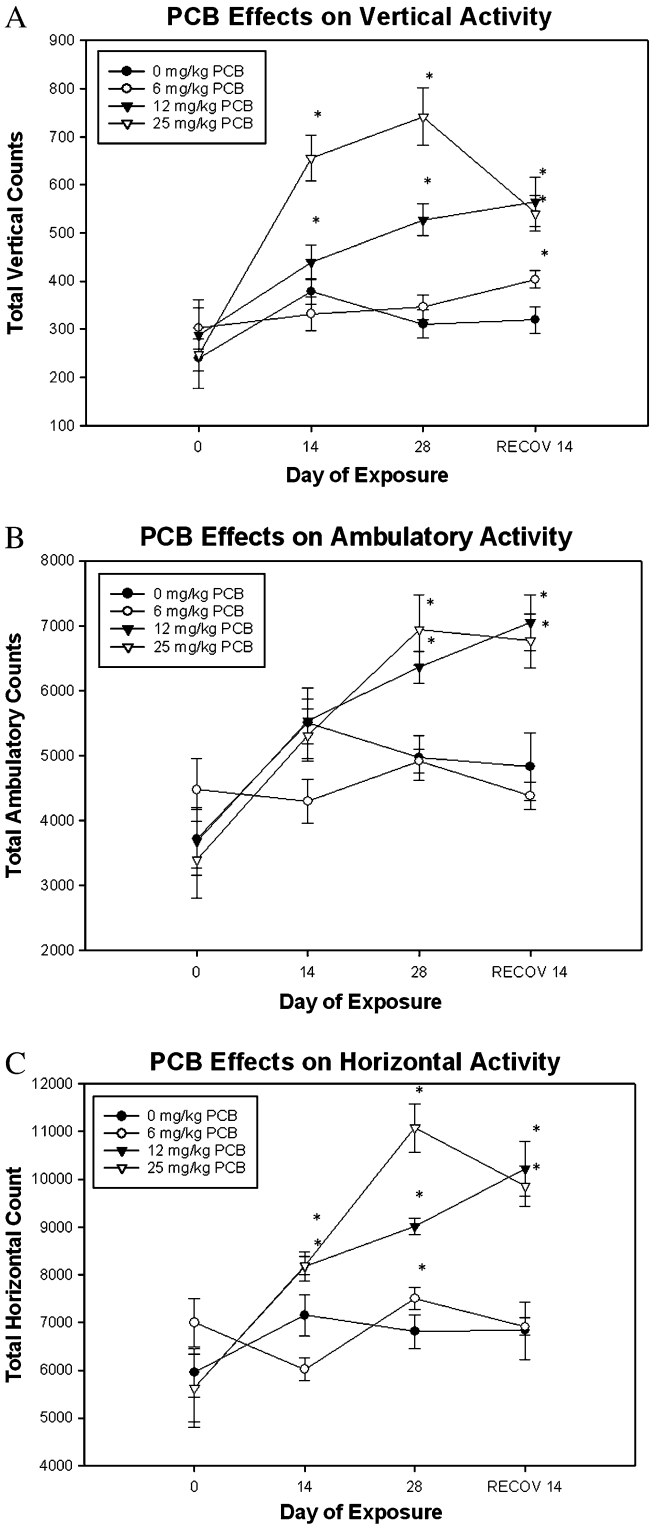

FIG. 2. PCB exposure elicits hyperactivity. Total vertical (A), ambulatory (B), and horizontal (C) locomotor activities were measured in mice exposed to vehicle or 6–25 mg/kg A1254. Data represent total activity counts ± SEM ($n = 10$) at week 0 (baseline) and at the end of exposure weeks 2, 4, and 2 weeks postexposure. *Denotes significant differences ($p < 0.0001$) from vehicle control at the same time point by repeated measures ANOVA.

Although exposure to 6 mg/kg A1254 led to a decrease in ambulation at the end of 2 weeks of exposure, mice in that dose group did not differ significantly from vehicle-control groups with time. Exposure to 12 and 25 mg/kg A1254 produced significant increase in ambulatory activity at the end of the 4-week exposure, which persisted for 2 weeks thereafter (Fig. 2B; main effect of exposure $F_{3,99} = 5.159$, $p = 0.0049$ and interaction effect of time and exposure $F_{3,99} = 3.827$, $p = 0.0004$). Significant alterations in horizontal activity were observed in by week 2 of PCB exposure. Mice exposed to 12 and 25 mg/kg A1254 exhibited sustained elevations in horizontal activity (Fig. 2C; main effect of exposure $F_{3,102} = 12.958$, $p < 0.0001$ and interaction effect of time and exposure $F_{3,102} = 7.171$, $p < 0.0001$). These findings demonstrate that PCB exposure also produces significant and persistent hyperactivity in adult mice in the higher dose groups.

Total Striatal Dopamine Was Elevated Following PCB Exposure

To determine if DA and metabolite levels were disrupted following PCB exposure at levels lower than previously examined, changes in striatal DA, its metabolites DOPAC and HVA, and DA turnover (DOPAC + HVA/DA) were evaluated at 2 weeks after the last exposure (Fig. 3). Although alterations in DA metabolites (DOPAC + HVA) and DA turnover were not observed with PCB exposure, DA levels increased by ~30% within each A1254 dose group (Fig. 3; $*p < 0.001$ and $\#p < 0.05$).

PCB Exposure Reduces Neuronal Cell Number in the SNpc and VTA

To determine if subchronic A1254 exposure (6–25 mg/kg) would cause cell loss in midbrain DAergic systems, mice were perfused 2 weeks following the last exposure, and VMB neurons were quantified by stereological cell counting. Moderate to high doses of A1254 elicited death of both TH+ and TH− cells in the VTA (Fig. 4A; $\#p < 0.01$, $+p < 0.001$, and $*p < 0.0001$ from control; $^{a}p < 0.01$ and $^{b}p < 0.0001$ from 6 mg/kg A1254; and $^{c}p < 0.001$ from 12 mg/kg A1254), by ~15–25% and ~15–35%, respectively. However, in the SNpc, only TH+ cells were significantly decreased, by ~15%, following the lowest dose of 6 mg/kg A1254 (Fig. 4B; $\#p < 0.01$). At the moderate and high doses, TH+ cells in the SNpc declined by ~20–30% (Fig. 4B; $+p < 0.001$ and $*p < 0.0001$ from control and $^{a}p < 0.05$ from 6 mg/kg A1254). Additionally, TH− cells of the SNpc decreased by 30%, but only in the highest dose group (Fig. 4B; $*p < 0.0001$ from control and $^{b}p < 0.005$ from 6 and 12 mg/kg A1254).

PCB Exposure Reduced TH and DAT Expression Within Striatum

Because we observed elevated DA levels but reductions in cell number in the VMB DAergic system following PCB exposure, TH and DAT expression was assessed to examine DAergic synaptic terminal integrity in the striatum (STR).

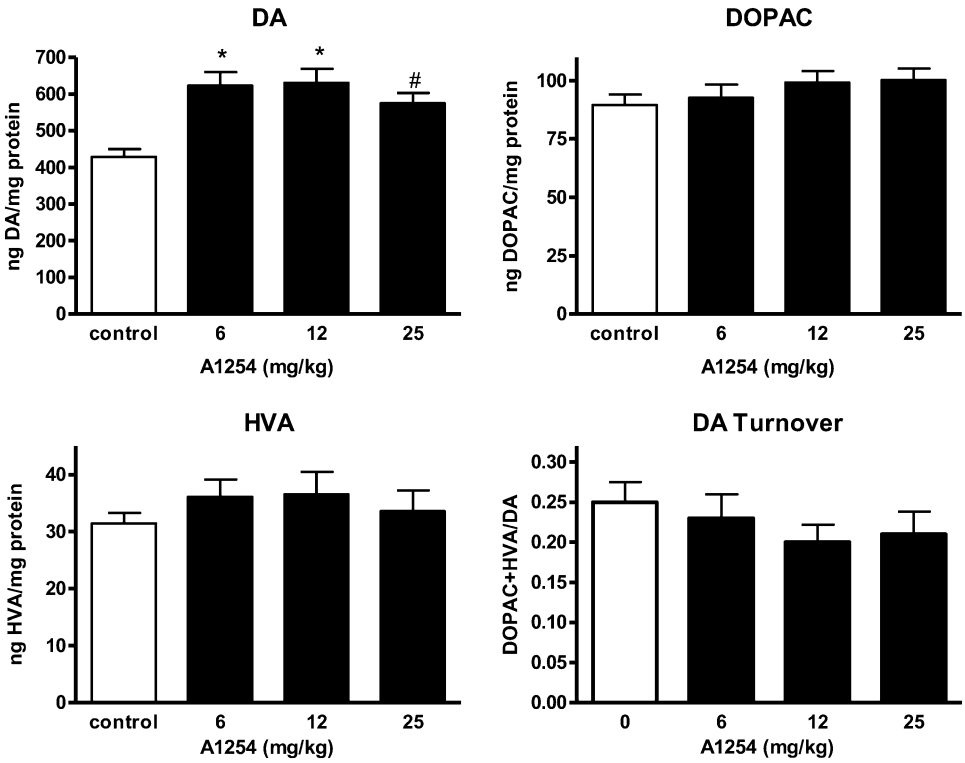

FIG. 3. Dopamine levels are elevated following PCB exposure. Striatal levels of dopamine (DA), DOPAC, HVA, and DA turnover (DOPAC + HVA)/DA were measured in tissue collected 2 weeks following a 28-day exposure to soybean oil vehicle or 6–25 mg/kg A1254 (mean ± SEM; $n = 10$). *$p < 0.001$ and #$p < 0.05$ from vehicle control.

A1254 exposure was associated with a modest (20%) but significant decrease in striatal TH levels in all exposure groups, as compared with controls (Figs. 5A and B; #$p < 0.05$). DAT levels were reduced by ~ 25–50% in a dose-dependent manner (Figs. 5C and D; #$p < 0.05$, *$p < 0.01$, and **$p < 0.001$), similar to previous observations (Caudle *et al.*, 2006).

PCB Exposure Generates Lipid Peroxidation Products and Oxidizes Protein In Vivo

Our previous studies (Lee and Opanashuk, 2004) indicated that A1254 generated a persistent OS response in DAergic neurons in culture. To further evaluate the potential roles of free radicals in cellular damage, brain tissue samples were assayed for MDA and 4-HNE, which are markers of oxidized lipids (Fig. 6A). Elevated MDA and 4-HNE (Fig. 6A; #$p < 0.05$) were detected in both the striatum and cerebellum. Furthermore, the extent of accumulation was greater in the striatum (42.9% over vehicle) compared with the cerebellum (26.6% over vehicle) of mice exposed to the mid-dose of PCBs (12 mg/kg). PCB-induced damage to proteins was determined by measuring protein carbonyl content, which is derived from the oxidation of amino acid side chains of aldehydes and ketones by ROS. OxyBlot analysis indicated that a greater number of proteins within a wide molecular weight range (~12, 25, 32, 45, 58, and 111 KDa) were oxidized in the striatum and cerebellum of PCB-exposed mice, compared with their respective vehicle controls (Fig. 6B; #$p < 0.05$, *$p < 0.01$, and **$p < 0.001$ from vehicle-exposed group; $^{a}p < 0.01$ from 6 mg/kg A1254, $^{b}p < 0.001$ from 6 mg/kg A1254; and $^{c}p < 0.05$ from 12 mg/kg A1254). These data indicate that subchronic PCB exposure for 4 weeks generates the formation of ROS, which can damage lipids and proteins within the brain.

OS-Related Protein Expression is Elevated in the Striatum and Cerebellum Following PCB Exposure

Previous studies in our laboratory indicated several protein alterations as a result of PCB exposure in an *in vitro* DAergic cell model, whereby a 10–30% depletion in mitochondrial MnSOD and a 125% increase in HO-1 were observed (Lee and Opanashuk, 2004). This study sought to further evaluate the OS response *in vivo* following PCB exposure. Striatal and cerebellar regions were collected and processed for 2D protein analysis for various antioxidant (SODs) and OS-related (HO-1) enzymes. Initial silver stained gels of striatal tissue lysates collected and processed from mice exposed to 0 and 25 mg/kg of A1254 revealed a global change in the expression of several proteins (Fig. 7A).

Using a more targeted approach, 2D and immunoblot analyses revealed a significant increase of proteins involved in cellular antioxidant defense strategies. HO-1 protein expression was elevated in the striatum (Fig. 7B) at 7 days for all PCB groups

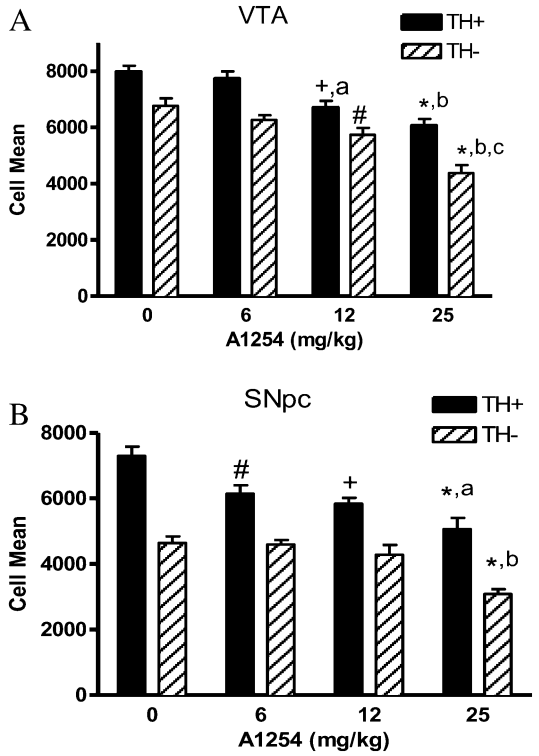

FIG. 4. Neurons are lost in the SNpc and VTA following PCB exposure. TH-positive (TH+) and TH-negative (TH−) DAergic neurons were counted from (A) SNpc sections taken from vehicle, 6, 12, and 25 mg/kg A1254-exposed mice 2 weeks following a 28-day exposure period (mean ± SEM; $n = 7$–8) #$p < 0.01$, +$p < 0.001$, and $p < 0.0001$ from control; [a]$p < 0.05$ from 6 and 12 mg/kg A1254; and [b]$p < 0.005$ from 6 and 12 mg/kg A1254 and (B) VTA sections taken from vehicle, 6, 12, and 25 mg/kg A1254-treated mice (mean ± SEM; $n = 7$–8). #$p < 0.01$, +$p < 0.01$, and *$p < 0.0001$ from control; [a]$p < 0.01$ and [b]$p < 0.0001$ from 6 mg/kg A1254; and [c]$p < 0.001$ from 12 mg/kg A1254.

($p = 0.0034$) and persisted at the 2-week time point following cessation of the 28-day PCB exposure. Moreover, HO-1 protein expression was significantly elevated in all dose groups compared with vehicle controls ($p = 0.0114$). Striatal MnSOD protein expression (Fig. 7C, top panel) was also elevated in a dose-dependent manner at 7 days ($p < 0.0001$), 14 days ($p = 0.0003$), 28 days ($p = 0.0008$; data not shown) of PCB exposure, and 2 weeks after exposure was terminated. Increased expression of CuZnSOD in the striatum (Fig. 7C, bottom panel) was modest, though significant at 14 days ($p = 0.0002$) and 28 days ($p < 0.0001$; data not shown) of PCB exposure, compared with HO-1 and MnSOD. Similarly, within the cerebellum, HO-1 protein expression at 7 days was elevated at all doses and at 14-day post-PCB exposure for the highest dose given (Fig. 7B). The cerebellar SODs (Mn and CuZn) also exhibited dose-dependent increases in protein expression with significance after 7 days of 25 mg/kg PCB exposure (Fig. 7C).

PCB Exposure Alters Iron Levels in the Brain

Previous studies imply that iron might participate in PCB-induced toxicity (Smith *et al.*, 1995; Whysner and Wang, 2001) and particularly in DA neuronal injury (Molina-Holgado *et al.*, 2008; Zhang *et al.*, 2005). Therefore, total iron (bound and unbound) in brain tissue following PCB exposure was measured by atomic absorption spectroscopy (Fig. 8A). Elevated iron levels were detected in the striatum ($p < 0.05$) at 7 days following 25 mg/kg A1254 PCB and 2 weeks after exposure ceased (Fig. 8A, top panel). Cerebellar iron levels initially decreased with 12 and 25 mg/kg A1254 after the first week of PCB exposure ($p < 0.05$) but returned to control levels after 28 days of exposure and 2 weeks thereafter (Fig. 8A; lower panel). Additionally, to determine the localization of free nonheme redox-active iron, a modified Perl's stain was utilized (Fig. 8B). A greater number of iron-positive cells were detected within the striatum and VMB with 25 mg/kg A1254 exposure. However, differences in Fe staining patterns were not observed in cerebellar tissue sections (data not shown).

Iron Regulatory Protein Expression Is Altered Following PCB Exposure

To determine the potential mechanism underlying the elevation in striatal iron at 7- and 14-day post-PCB exposure, immunoblot analyses were performed targeting TfR and ferritin as potential contributors to this iron overload. Although ferritin levels were initially increased threefold following PCB exposure (Fig. 9A), levels dropped to less than control 14 days following termination of 25 mg/kg PCB exposure ($p < 0.05$). Additionally, the iron influx protein TfR was dramatically increased sixfold following 28-day PCB exposure (Fig. 9B; $p < 0.001$) and returned to baseline levels 14 days after exposure was terminated.

DISCUSSION

Our data indicated that abnormal DA homeostasis, OS, and iron dysregulation potentially contribute to the molecular mechanisms involved in behavioral abnormalities and neuronal cell death following PCB exposure. Whereas striatal DA levels were elevated, DAT and TH expression were significantly reduced. Moreover, PCB-exposed mice exhibited alterations in several antioxidant enzyme levels coincidentally with increases in oxidatively modified lipids and proteins within the striatum and cerebellum. Iron accumulation was also observed in the striatum and midbrain along with abnormal striatal ferritin and transferrin receptor expression following PCB exposure, suggesting that both iron storage and transport processes were compromised.

Previous studies have shown that PCB congeners are widely distributed in rat brain following gestational or adult exposure to Aroclor mixtures (Kodavanti *et al.*, 1998; Ness *et al.*, 1994) and that PCBs accumulate in rat neuronal cells following A1254 exposure *in vitro* (Meacham *et al.*, 2005). Among the most abundant congeners were PCBs 105, 118, 138 + 163, 153 + 132, and 180, which are all noncoplanar (*ortho* substituted) and have consistently been reported to be more neurotoxic than the coplanar compounds (Mariussen *et al.*, 1999; Wong *et al.*,

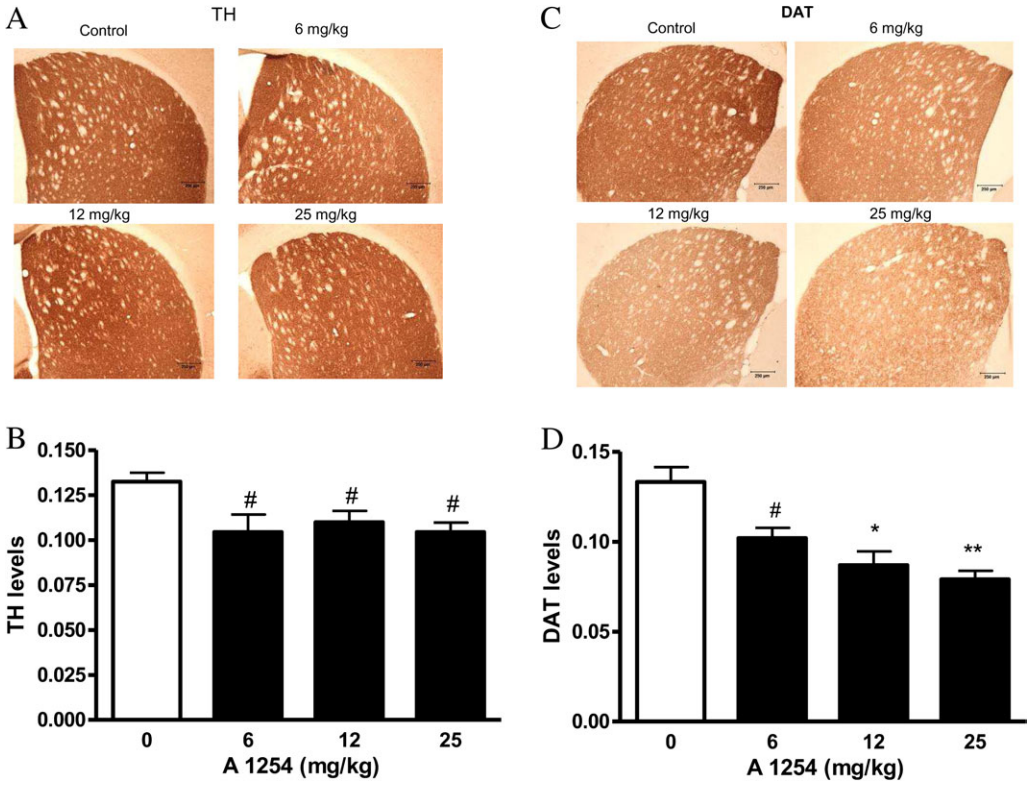

FIG. 5. DAT levels and TH levels decline following PCB exposure. Thirty micrometer striatal sections were stained from vehicle (soybean oil) and A1254-exposed (6–25 mg/kg) mice 2 weeks after a 28-day exposure period for TH (A) and DAT (C) by immunohistochemistry. Staining levels were quantified by densitometry for TH (B) and DAT (D). #$p < 0.05$, +$p < 0.01$, and *$p < 0.001$ from vehicle control.

1997). PCB congeners were widely distributed throughout several brain regions including the midbrain and striatum (Fig. 1). Interestingly, a previous study in humans revealed that PCBs accumulated in the striatum of postmortem PD brains, suggesting that organochlorine exposure might be involved in neurodegeneration (Corrigan *et al.*, 1998). The deposition of multiple congeners within brain regions that control movement, such as the DAergic system, underscores the need to further investigate the mechanisms by which PCB exposure disrupts normal motor function.

Considering that DA neurons in the SN and VTA were lost following PCB exposure, it would have been expected that striatal DA levels might have also declined. Instead, total DA levels increased, but DA turnover and metabolite levels were not altered following PCB exposure (Fig. 3). Our neurochemical data are contradictory to previous studies that have reported reduced DA levels following PCB exposure (Bemis and Seegal, 1999; Seegal *et al.*, 1994). One potential explanation is the limitations of the HPLC method, which only measures total cellular DA and its metabolites without providing information on extracellular levels. Accordingly, a previous *in vivo* microdialysis study (Seegal *et al.*, 2002) demonstrated that exposure to 25 mg/kg A1254 elicited time-dependent elevations in extraneuronal striatal DA in adult rats, without concomitant changes in total tissue DA levels. In our study, the elevated DA could be explained by a compensatory increase in TH activity despite modest decreases in striatal TH and DAT protein expression. These findings are consistent with a previous study that reported diminished striatal DAT expression and DA uptake by DAT following a similar PCB exposure regimen (Caudle *et al.*, 2006). Therefore, it is possible that striatal DA is elevated because presynaptic uptake is reduced, and synthesis is spared irrespective of neuron loss in the VMB.

We observed a significant loss of non-DAergic neurons within the SNpc and VTA (Fig. 4) after exposure to 25 mg/kg A1254. The nigrostriatal and mesolimbic pathways require not only DA but also additional neurotransmitters to coordinate function. For example, an imbalance between DAergic and noradrenergic systems has been implicated as a potential regulator of hyperactivity in mice (Jones and Hess, 2003). The degeneration of striatal GABAergic neurons has also been suggested to play a role in motor dysfunction observed in mice that exhibited a persistent elevation in extracellular DA (Cyr *et al.*, 2003). Moreover, lesions of DAergic projections from the VTA to the prefrontal cortex have been shown to produce hyperactivity (Viggiano *et al.*, 2003). Although our studies imply that PCB-induced loss of both DAergic and other

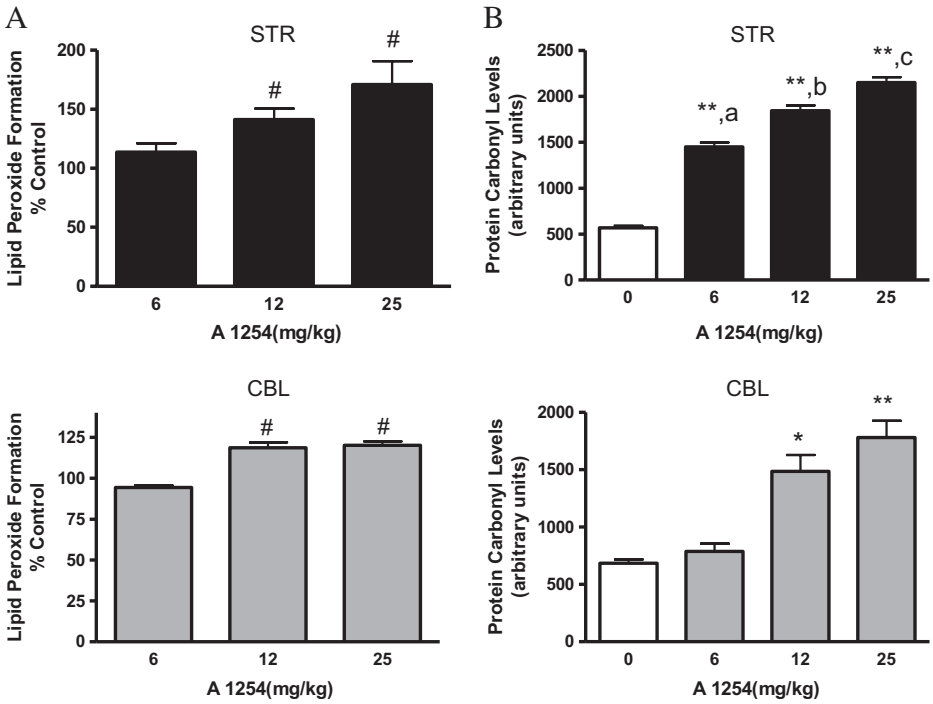

FIG. 6. Lipid peroxidation products accumulate and protein carbonyls are elevated in striatum and cerebellum following PCB exposure. Striatal and cerebellar tissues were analyzed for lipid peroxidation (A) or protein carbonyl formation (B) at 2 weeks after a 28-day exposure to vehicle or 6–25 mg/kg A1254 (mean ± SEM; $n = 5$) in tissue lysates. #$p < 0.05$, *$p < 0.01$, and **$p < 0.001$ from vehicle-exposed group; [a]$p < 0.01$ from 6 mg/kg A1254; [b]$p < 0.001$ from 6 mg/kg A1254; and [c]$p < 0.05$ from 12 mg/kg A1254. The control values (micromolar per milligram protein ± SEM) for lipid peroxidation products were 3.88 ± 0.75 (STR) and 3.23 ± 0.63 (CBL).

neurons in the VMB contribute to hyperactivity, the particular mechanisms of neurotoxicity remain to be defined.

Dopaminergic neurons are particularly susceptible to OS due to the intrinsic oxidative nature of DA itself, which can be degraded both enzymatically by the monoamine oxidases and nonenzymatically by autoxidation. These metabolic processes give rise to free radical byproducts, making it plausible that sustained OS in DAergic pathways mediates PCB neurotoxicity. We detected increases in both the accumulation of lipid peroxidation products (Fig. 6A) and oxidatively modified proteins (Fig. 6B) in striatum as well as cerebellum from mice exposed to PCBs. These brain regions were chosen based on their involvement in the regulation of motor movement as well as their intrinsic difference in the composition of dopaminergic neurons. However, because whole tissue lysates were analyzed for OS-derived proteins and lipids, it was not possible to identify the precise neuronal cell populations within each region that were impacted by PCB exposure. Nevertheless, our studies are consistent with a role for the imbalance between ROS production and antioxidant defense systems in PCB neurotoxicity *in vivo*.

Several antioxidant protein levels were altered in both striatum and cerebellum from PCB-exposed mice following PCB exposure (Figs. 7B and C). The upregulation of CuZnSOD and MnSOD protein expression provides a first line of defense against superoxide anion production (Fridovich, 1978), which has been demonstrated in cellular injury models (Takeuchi *et al.*, 2000). Increases in both SOD proteins (Fig. 7C) suggest that PCB exposure elicits a cellular compartmentalization of OS via superoxide anion production in both the mitochondria and cytoplasm of cells within the striatum and cerebellum. Elevated striatal HO-1 levels after 7 days of PCB exposure is consistent with an adaptive role for this antioxidant enzyme as an early stress response protein (Dennery, 2000). The persistent HO-1 protein expression after exposure was terminated suggests that striatal cells are experiencing chronic OS. The induction of HO-1 observed at the earliest time point potentially indicates a role of HO-1 being an early response stress protein. However, sustained HO-1 expression suggests that cells within these brain areas are undergoing chronic OS. Therefore, we speculate that in addition to offering protection against PCBs, HO-1 could participate in mediating oxidative injury, perhaps through excessive iron levels generated as a byproduct of enhanced enzyme activity, as suggested by our *in vitro* studies (Lee *et al.*, 2006).

Iron dysregulation is a consistent feature of neurodegenerative disorders, and studies have shown that selective DAergic cell loss correlates with elevated levels of intracellular iron in PD (Dexter *et al.*, 1989; Riederer *et al.*, 1992). In our study, mice exposed to 25 mg/kg A1254 accumulated significantly higher iron levels in striatum at day 7 and 2 weeks after exposure ended (Fig. 8A), suggesting that impaired iron homeostasis persists. Considering the oxidative environment of DAergic neurons, if redox-active iron is not properly

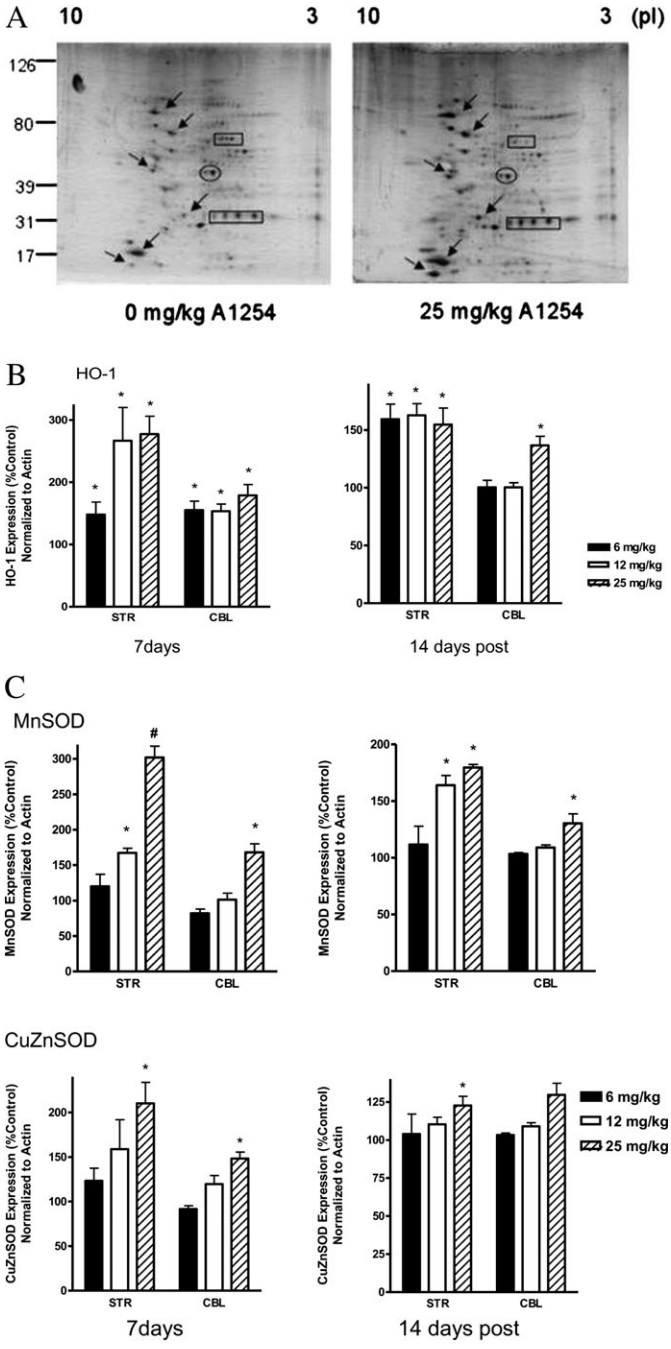

FIG. 7. HO-1, MnSOD, and CuZnSOD protein levels are more abundant in the striatum and cerebellum following PCB exposure. Striatal and cerebellar protein lysates were processed for 2D-IEF/SDS-PAGE following a 4-week PCB exposure (0–25 mg/kg A1254) and a 2-week recovery period. PVDF membranes (A) were immunoblotted for HO-1, MnSOD, and CuZnSOD (arrows). Membranes were probed with an antibody specific for actin to control for equal loading. Immunopositive spots from three different blots were quantified with Quantity One analysis program (Bio-Rad) for HO-1 (B) and the SOD proteins (C). Bars represent the mean ± SEM expressed as a percent of vehicle control. $*p < 0.005$ and $\#p < 0.0001$ from vehicle control.

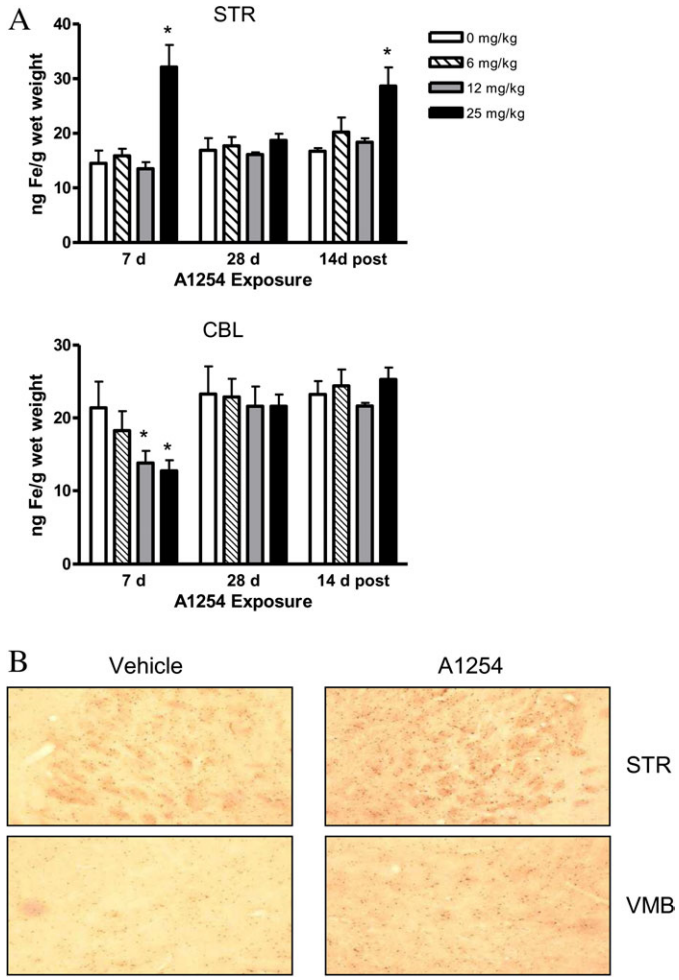

FIG. 8. Total iron levels are elevated in striatum following PCB exposure. (A) Striatal and cerebellar tissue were analyzed for total iron levels by atomic absorption spectroscopy (mean ± SEM; $n = 4$). $*p < 0.05$ from vehicle-control groups by ANOVA. (B) 30 μm sections of the striatum (STR) and midbrain (MB) were processed for Perl's staining and visualized microscopically. Representative brain sections ($n = 3$ per exposure group) are shown here.

buffered, there is enhanced potential for nerve terminal injury in the striatum, which could lead to cell body loss in the midbrain. Enhanced iron staining was also observed in the striatum and midbrain from PCB-exposed mice, implying that iron plays a role in PCB neurotoxicity within these brain regions. However, the absence of iron accumulation within the CBL does not preclude the generation of oxidative events following PCB exposure, as evidenced by the elevated oxidatively modified protein and lipid levels (Fig. 6), as well as elevated OS-related protein expression (Fig. 7). In striatum, the initial increase in ferritin is presumably an adaptive response, via inactivation of iron-regulatory proteins (Ponka *et al.*, 1998), to excess intracellular iron (Fig. 9A). The ultimate decrease in iron storage 2 weeks following exposure cessation could indicate an overburdening of sequestration capabilities. Additionally, the elevated TfR expression at 28 days of PCB exposure may reflect an opportunity for enhanced iron uptake into the cells, which together with a decrease in iron storage by

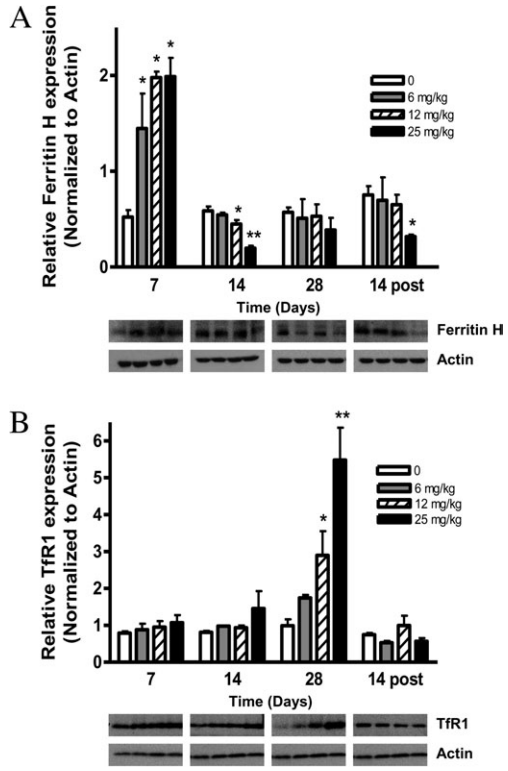

FIG. 9. PCB exposure increases transferrin receptor (TfR1) protein levels, while reducing ferritin-H protein levels in the striatum. Striatal protein lysates were processed for SDS-PAGE following a 4-week PCB exposure (0–25 mg/kg A1254) and a 2-week recovery period. PVDF membranes were immunoblotted for (A) Ferritin H and (B) TfR1. Membranes were probed with a β-actin antibody to control for equal loading. Densitometric values were acquired using Image J software (mean ± SEM; $n = 3$). *$p < 0.05$ and **$p < 0.001$ from vehicle control.

ferritin would lead to iron overload in the cells (Gerlach *et al*., 2006; Lu *et al*., 1989), consistent with our data obtained by atomic absorption spectroscopy and Perl's staining (Figs. 8A and B). Whereas prior studies have implicated iron in the promotion of carcinogenicity induced by PCB exposure (Faux *et al*., 1992; Madra *et al*., 1996; Smith *et al*., 1995), our work suggests that impaired iron homeostasis and ROS contribute to PCB neurotoxicity.

OS and elevated iron levels have been linked to the pathophysiology of several neurodegenerative disorders, such as PD. Accumulating evidence suggests that PD-related neurodegeneration results from the interplay between genetic susceptibilities, environmental factors, and the normal aging process. Therefore, the identification of subtle biological effects following persistent low-level PCB exposure might offer insight into the vulnerability of the CNS to neurodegenerative events associated with OS and iron dysregulation. Although the sources of ROS and elevated iron levels following PCB exposure remain unknown, it is speculated that OS serves as a primary mechanism in the neurodegeneration of DAergic pathways following PCB exposure. Although it is difficult to extrapolate the relevance of the present findings to human health, there is evidence from this study as well as findings from Caudle *et al*. (2006) that confirm exposure levels in mouse brains comparable with those found in human postmortem brain tissues (Dewailly *et al*., 1999). These exposure levels were correlative with significant changes to the nigrostriatal DA pathway, consistent with some models of neurodegeneration and provide widespread implications for oxidative injury throughout the brain following long-term low-level PCB exposure. Therefore, understanding the role of redox imbalance and abnormal iron homeostasis in PCB-induced neuronal injury could have global implications for the pathogenesis of Parkinsonism and other disorders associated with DA system dysfunction.

FUNDING

National Institutes of Health (K22 ES00375, P30 ES01247, and T32 ES07026).

ACKNOWLEDGMENTS

We thank Bryan Thompson for technical and editorial assistance.

REFERENCES

Bemis, J. C., and Seegal, R. F. (1999). Polychlorinated biphenyls and methylmercury act synergistically to reduce rat brain dopamine content in vitro. *Environ. Health Perspect.* **107,** 879–885.

Bemis, J. C., and Seegal, R. F. (2004). PCB-induced inhibition of the vesicular monoamine transporter predicts reductions in synaptosomal dopamine content. *Toxicol. Sci.* **80,** 288–295.

Berman, S. B., and Hastings, T. G. (1999). Dopamine oxidation alters mitochondrial respiration and induces permeability transition in brain mitochondria: Implications for Parkinson's disease. *J. Neurochem.* **73,** 1127–1137.

Caudle, W. M., Richardson, J. R., Delea, K. C., Guillot, T. S., Wang, M., Pennell, K. D., and Miller, G. W. (2006). Polychlorinated biphenyl-induced reduction of dopamine transporter expression as a precursor to Parkinson's disease-associated dopamine toxicity. *Toxicol. Sci.* **92,** 490–499.

Corrigan, F. M., Murray, L., Wyatt, C. L., and Shore, R. F. (1998). Diorthosubstituted polychlorinated biphenyls in caudate nucleus in Parkinson's disease. *Exp. Neurol.* **150,** 339–342.

Cyr, M., Beaulieu, J. M., Laakso, A., Sotnikova, T. D., Yao, W. D., Bohn, L. M., Gainetdinov, R. R., and Caron, M. G. (2003). Sustained elevation of extracellular dopamine causes motor dysfunction and selective degeneration of striatal GABAergic neurons. *Proc. Natl. Acad. Sci. U.S.A.* **100,** 11035–11040.

Dennery, P. A. (2000). Regulation and role of heme oxygenase in oxidative injury. *Curr. Top. Cell. Regul.* **36,** 181–199.

Dewailly, E., Mulvad, G., Pedersen, H. S., Ayotte, P., Demers, A., Weber, J. P., and Hansen, J. C. (1999). Concentration of organochlorines in human brain, liver, and adipose tissue autopsy samples from Greenland. *Environ. Health Perspect.* **107,** 823–828.

Dexter, D. T., Wells, F. R., Lees, A. J., Agid, F., Agid, Y., Jenner, P., and Marsden, C. D. (1989). Increased nigral iron content and alterations in other metal ions occurring in brain in Parkinson's disease. *J. Neurochem.* **52,** 1830–1836.

Faux, S. P., Francis, J. E., Smith, A. G., and Chipman, J. K. (1992). Induction of 8-hydroxydeoxyguanosine in Ah-responsive mouse liver by iron and Aroclor 1254. *Carcinogenesis* **13,** 247–250.

Fridovich, I. (1978). Superoxide dismutases: Defence against endogenous superoxide radical. *Ciba Found. Symp.* **65,** 77–93.

Gerlach, M., Double, K. L., Youdim, M. B., and Riederer, P. (2006). Potential sources of increased iron in the substantia nigra of parkinsonian patients. *J. Neural Transm. Suppl.* **70,** 133–142.

Graham, D. G. (1978). Oxidative pathways for catecholamines in the genesis of neuromelanin and cytotoxic quinones. *Mol. Pharmacol.* **14,** 633–643.

Greizerstein, H. B., Gigliotti, P., Vena, J., Freudenheim, J., and Kostyniak, P. J. (1997). Standardization of a method for the routine analysis of polychlorinated biphenyl congeners and selected pesticides in human serum and milk. *J. Anal. Toxicol.* **21,** 558–566.

Gwiazda, R. H., Lee, D., Sheridan, J., and Smith, D. R. (2002). Low cumulative manganese exposure affects striatal GABA but not dopamine. *Neurotoxicology* **23,** 69–76.

Halliwell, B. (1992). Reactive oxygen species and the central nervous system. *J. Neurochem.* **59,** 1609–1623.

Hsu, S. T., Ma, C. I., Hsu, S. K., Wu, S. S., Hsu, N. H., Yeh, C. C., and Wu, S. B. (1985). Discovery and epidemiology of PCB poisoning in Taiwan: A four-year followup. *Environ. Health Perspect.* **59,** 5–10.

Jenner, P. (1996). Oxidative stress in Parkinson's disease and other neurodegenerative disorders. *Pathol. Biol.* **44,** 57–64.

Jones, M. D., and Hess, E. J. (2003). Norepinephrine regulates locomotor hyperactivity in the mouse mutant coloboma. *Pharmacol. Biochem. Behav.* **75,** 209–216.

Kashimoto, T., Miyata, H., Kunita, S., Tung, T. C., Hsu, S. T., Chang, K. J., Tang, S. Y., Ohi, G., Nakagawa, J., and Yamamoto, S. (1981). Role of polychlorinated dibenzofuran in yusho (PCB poisoning). *Arch. Environ. Health* **36,** 321–326.

Kodavanti, P. R. S., Kannan, N., Yamashita, N., Derr-Yellin, E. C., Ward, T. R., Burgin, D. E., Tilson, H. A., and Birnbaum, L. S. (2001). Differential effects of two lots of Aroclor 1254: Congener-specific analysis and neurochemical end points. *Environ. Health Perspect.* **109,** 1153–1161.

Kodavanti, P. R. S., Ward, T. R., Derr-Yellin, E. C., Mundy, W. R., Casey, A. C., Bush, B., and Tilson, H. A. (1998). Congener-specific distribution of polychlorinated biphenyls in brain regions, blood, liver, and fat of adult rats following repeated exposure to Aroclor 1254. *Toxicol. Appl. Pharmacol.* **153,** 199–210.

Lee, D. W., Gelein, R. M., and Opanashuk, L. A. (2006). Heme-oxygenase-1 promotes polychlorinated biphenyl mixture Aroclor 1254-induced oxidative stress and dopaminergic cell injury. *Toxicol. Sci.* **90,** 159–167.

Lee, D. W., and Opanashuk, L. A. (2004). Polychlorinated biphenyl mixture Aroclor 1254-induced oxidative stress plays a role in dopaminergic cell injury. *Neurotoxicology* **25,** 925–939.

Lu, J. P., Hayashi, K., and Awai, M. (1989). Transferrin receptor expression in normal, iron-deficient and iron-overloaded rats. *Acta Pathol. Jpn.* **39,** 759–764.

Madra, S., Mann, F., Francis, J. E., Manson, M. M., and Smith, A. G. (1996). Modulation by iron of hepatic microsomal and nuclear cytochrome P450, and cytosolic glutathione S-transferase and peroxidase in C57BL/10ScSn mice induced with polychlorinated biphenyls (Aroclor 1254). *Toxicol. Appl. Pharmacol.* **136,** 79–86.

Mariussen, E., Morch Andersen, J., and Fonnum, F. (1999). The effect of polychlorinated biphenyls on the uptake of dopamine and other neurotransmitters into rat brain synaptic vesicles. *Toxicol. Appl. Pharmacol.* **161,** 274–282.

Meacham, C. A., Freudenrich, T. M., Anderson, W. L., Sui, L., Lyons-Darden, T., Barone, S., Jr, Gilbert, M. E., Mundy, W. R., and Shafer, T. J. (2005). Accumulation of methylmercury or polychlorinated biphenyls in in vitro models of rat neuronal tissue. *Toxicol. Appl. Pharmacol.* **205,** 177–187.

Molina-Holgado, F., Gaeta, A., Francis, P. T., Williams, R. J., and Hider, R. C. (2008). Neuroprotective actions of deferiprone in cultured cortical neurones and SHSY-5Y cells. *J. Neurochem.* **105,** 2466–2476.

Ness, D. K., Schantz, S. L., and Hansen, L. G. (1994). PCB congeners in the rat brain: Selective accumulation and lack of regionalization. *J. Toxicol. Environ. Health* **43,** 453–468.

Palmer, C., Menzies, S. L., Roberts, R. L., Pavlick, G., and Connor, J. R. (1999). Changes in iron histochemistry after hypoxic-ischemic brain injury in the neonatal rat. *J. Neurosci. Res.* **56,** 60–71.

Petersen, M. S., Halling, J., Bech, S., Wermuth, L., Weihe, P., Nielsen, F., Jorgensen, P. J., Budtz-Jorgensen, E., and Grandjean, P. (2008). Impact of dietary exposure to food contaminants on the risk of Parkinson's disease. *Neurotoxicology* **29,** 584–590.

Ponka, P., Beaumont, C., and Richardson, D. R. (1998). Function and regulation of transferrin and ferritin. *Semin. Hematol.* **35,** 35–54.

Riederer, P., Dirr, A., Goetz, M., Sofic, E., Jellinger, K., and Youdim, M. B. (1992). Distribution of iron in different brain regions and subcellular compartments in Parkinson's disease. *Ann. Neurol.* **32**(Suppl), S101–S104.

Rousselet, E., Joubert, C., Callebert, J., Parain, K., Tremblay, L., Orieux, G., Launay, J. M., Cohen-Salmon, C., and Hirsch, E. C. (2003). Behavioral changes are not directly related to striatal monoamine levels, number of nigral neurons, or dose of parkinsonian toxin MPTP in mice. *Neurobiol. Dis.* **14,** 218–228.

Seegal, R. F. (1994). The neurochemical effects of PCB exposure are age-dependent. *Arch. Toxicol. Suppl.* **16,** 128–137.

Seegal, R. F., Bush, B., and Brosch, K. O. (1994). Decreases in dopamine concentrations in adult, non-human primate brain persist following removal from polychlorinated biphenyls. *Toxicology* **86,** 71–87.

Seegal, R. F., Okoniewski, R. J., Brosch, K. O., and Bemis, J. C. (2002). Polychlorinated biphenyls alter extraneuronal but not tissue dopamine concentrations in adult rat striatum: An in vivo microdialysis study. *Environ. Health Perspect.* **110,** 1113–1117.

Smith, A. G., Carthew, P., Clothier, B., Constantin, D., Francis, J. E., and Madra, S. (1995). Synergy of iron in the toxicity and carcinogenicity of polychlorinated biphenyls (PCBs) and related chemicals. *Toxicol. Lett.* **82–83,** 945–950.

Smith, S. R., Cooperman, S., Lavaute, T., Tresser, N., Ghosh, M., Meyron-Holtz, E., Land, W., Ollivierre, H., Jortner, B., Switzer, R., III, *et al.* (2004). Severity of neurodegeneration correlates with compromise of iron metabolism in mice with iron regulatory protein deficiencies. *Ann. N. Y. Acad. Sci.* **1012,** 65–83.

Steenland, K., Hein, M. J., Cassinelli, R. T., II, Prince, M. M., Nilsen, N. B., Whelan, E. A., Waters, M. A., Ruder, A. M., and Schnorr, T. M. (2006). Polychlorinated biphenyls and neurodegenerative disease mortality in an occupational cohort. *Epidemiology* **17,** 8–13.

Takeuchi, A., Miyaishi, O., Kiuchi, K., and Isobe, K. (2000). Cu/Zn- and Mn-superoxide dismutases are specifically up-regulated in neurons after focal brain injury. *J. Neurobiol.* **45,** 39–46.

Thiruchelvam, M., McCormack, A., Richfield, E. K., Baggs, R. B., Tank, A. W., Di Monte, D. A., and Cory-Slechta, D. A. (2003). Age-related irreversible progressive nigrostriatal dopaminergic neurotoxicity in the paraquat and maneb model of the Parkinson's disease phenotype. *Eur. J. Neurosci.* **18,** 589–600.

Tilson, H. A., and Kodavanti, P. R. (1997). Neurochemical effects of polychlorinated biphenyls: An overview and identification of research needs. *Neurotoxicology* **18,** 727–743.

Tse, D. C., McCreery, R. L., and Adams, R. N. (1976). Potential oxidative pathways of brain catecholamines. *J. Med. Chem.* **19,** 37–40.

Viggiano, D., Ruocco, L. A., and Sadile, A. G. (2003). Dopamine phenotype and behaviour in animal models: In relation to attention deficit hyperactivity disorder. *Neurosci. Biobehav. Rev.* **27,** 623–637.

Whysner, J., and Wang, C. X. (2001). Hepatocellular iron accumulation and increased cell proliferation in polychlorinated biphenyl-exposed Sprague-Dawley rats and the development of hepatocarcinogenesis. *Toxicol. Sci.* **62,** 36–45.

Wong, P. W., Brackney, W. R., and Pessah, I. N. (1997). Ortho-substituted polychlorinated biphenyls alter microsomal calcium transport by direct interaction with ryanodine receptors of mammalian brain. *J. Biol. Chem.* **272,** 15145–15153.

Zhang, X., Xie, W., Qu, S., Pan, T., Wang, X., and Le, W. (2005). Neuroprotection by iron chelator against proteasome inhibitor-induced nigral degeneration. *Biochem. Biophys. Res. Commun.* **333,** 544–549.